

Numerical assessment of ion turbulent thermal transport scaling laws

M. Ottaviani^a, G. Manfredi^b

^a Département de Recherches sur la Fusion Contrôlée,
Commissariat à l'Energie Atomique, Centre de Cadarache,
Saint-Paul-lez-Durance

^b Laboratoire de Physique des Milieux Ionisés, Université Henri Poincaré, Nancy,
Vandoeuvre-les-Nancy
France

Abstract. Numerical simulations of ion temperature gradient driven turbulence are carried out to investigate the parametric dependence of ion thermal transport on the reduced gyroradius and on the local safety factor. Whereas the simulations show a clear proportionality of the conductivity to the gyroradius, the dependence on the safety factor cannot be represented as a simple power law like the one exhibited by the empirical scaling laws.

1. Introduction

The considerable amount of experimental data related to anomalous transport in tokamaks is commonly summarized in terms of empirical scaling laws [1]. Global quantities, such as the energy confinement time, are expressed as products of the main experimental control parameters, such as the input power and the plasma current, raised to certain exponents, which are determined empirically. While the power law form of the confinement law is chosen mainly for convenience, it is evidently rather restrictive. Indeed, the parametric dependence of the effective transport coefficients on the local variables need not be monomial (power law), or it may be so only as a function of certain quantities. Furthermore, different parts of the discharge may be dominated by different transport processes with different transport laws. Thus, global scaling laws may simply express average behaviour, and, while useful to identify general trends, for example for machine design, no special physical significance can be attached to the precise value of their exponents.

In the present situation, a valuable contribution to the understanding of anomalous transport can come from the detailed study of the scaling (or lack of scaling) properties of specific, relevant plasma dynamics models.

This is the goal of the present article, where some of the scaling properties of a model of the ion thermal transport caused by ion temperature gradient (ITG) driven turbulence are analysed.

Specifically, we investigate the dependence of the effective ion thermal conductivity on two key dimensionless parameters, the reduced gyroradius $\rho_* = \rho_s/a$ (ρ_s is the ion sound Larmor radius and a the minor radius) and the safety factor q . The importance of these two parameters in machine design is well known. The reduced gyroradius is the parameter that changes most when extrapolating from present day tokamaks to future larger machines. The difference in the predicted performance when extrapolating certain JET DT shots to (the old) ITER under two different ρ_* scaling laws is clearly illustrated in Ref. [2]. The interest in the q dependence comes from the fact that the confinement law exhibits a strong plasma current dependence, and it is therefore important to assess whether this corresponds to some local scaling dependence.

The latest numerical simulations, carried out at smaller ρ_* , show a clear proportionality of the conductivity to the gyroradius (gyro-Bohm scaling), which fully confirms the results of an earlier study [3]. On the other hand, it was found that the dependence on the safety factor cannot be represented as a simple power law like the one exhibited by the empirical scaling laws. An attempt to cast the current dependence as a power law gives an exponent that decreases with input power.

The article is organized as follows. First we present the model (Section 2) and review and update the ρ_* scaling study (Section 3), then we report on the current scaling studies (Section 4). A brief discussion and a summary are given in Section 5.

2. The model

The simulations discussed in this article were carried out with the code ETAI3D, which solves the minimal (paradigm) fluid model of ITG turbulence in a torus. The details of this code are given in Ref. [3]. Here we summarize the salient features. The model equations are

$$dw/dt - 2\epsilon\omega_d(\Phi + T_i) + A\nabla_{\parallel}v + (\kappa_n/r) \partial_{\theta}\Phi = D_w\nabla^2w - \gamma_{pdf}\langle w \rangle \quad (1)$$

$$dv/dt + A\nabla_{\parallel}(\Phi + T_i) = D_v\nabla^2v \quad (2)$$

$$dT_i/dt + \Gamma\langle T_i \rangle A\nabla_{\parallel}v = -A\langle T_i \rangle^{1/2}|\nabla_{\parallel}|T_i + D_T\nabla^2T_i \quad (3)$$

where $w = (\Phi - \langle \Phi \rangle)/T_e - \rho_*^2\nabla^2\Phi$ is the generalized vorticity (effectively the ion guiding centre density), Φ the electric potential, v the parallel ion velocity, T_i the ion temperature, $d/dt = \partial_t + \mathbf{v}_E \cdot \nabla$ the advection operator, $\omega_d = (1/r)(\cos\theta)\partial_{\theta} + (\sin\theta)\partial_r$ the curvature operator and $\nabla_{\parallel} = (1/q)(q\partial_{\phi} + \partial_{\theta})$ the parallel derivative operator, while $\langle \cdot \rangle$ denotes flux surface average, $A = \epsilon/\rho_*$ and Γ is a constant. Units of T_e for temperature, T_e/e for potential and $c_s = (T_e/M_i)^{1/2}$ for velocity are employed. Also note that large scale units, a (the minor radius) for lengths and $a^2/(cT_e/eB)$ for time, are used. Finally, D_w , D_v and D_T are small artificial perpendicular dissipation coefficients set to damp the smallest scales, and γ_{pdf} is a further coefficient introduced to model the poloidal flow damping. In the rest of this article, $\gamma_{pdf} = \epsilon/q\rho_*$, which scales like the ion transit frequency, when written in dimensional units.

Noteworthy features of this code are

- (a) Globality. The code solves the model equations, in toroidal geometry and in a domain between two arbitrary circular magnetic surfaces, without using the local or flux tube approximation. This is necessary in order to answer questions related to the $\rho_* = \rho_s/a$ scaling, without a priori assumptions about the scale separation.
- (b) Flux boundary conditions. The input power is given as a control parameter by specifying either the heat flux through the inner boundary or by a given power deposition profile. The (fluctuating) ion temperature is the outcome of the simulations. This is primarily done to avoid any assumption about the (unknown) time averaged profile and to allow quite naturally any

possible intermittent phenomena in the profile dynamics.

- (c) Emphasis on the mesoscale dynamics. As suggested by experiments, as well as by theoretical considerations, most of the turbulent energy accumulates in the spectral region around the poloidal and radial wavenumbers $k_{\theta}\rho_s \approx k_r\rho_s \sim 0.1$, which is where the turbulence is suppressed by Landau damping. This allows one to work with model equations that neglect most finite Larmor radius terms.
- (d) Emphasis on long timescales. Simulations are carried out for at least one global energy confinement time in most cases. The profiles shown in this article are time averages over (statistically) steady state turbulence. The duration of the simulations guarantees good statistics of the measured quantities, since, as it turns out, the ratio of the energy confinement time to the turbulence characteristic time(s) scales as ρ_*^{-2} .

All the studies presented in this article were carried out in the toroidal annulus between the magnetic surfaces at $r = 0.5$ and $r = 1$.

3. Gyroradius scaling

The first application has been to the problem of the ρ_* scaling of the ion conductivity. (Here the conductivity in a turbulent steady state is defined as the ratio of the time averaged heat flux to the time averaged temperature gradient.) In Bohm units ($\chi_B = cT_e/eB$) the ion conductivity χ_i scales like a power of ρ_* . In L mode tokamak operations, χ_i/χ_B seems almost ρ_* independent (Bohm scaling), while in H modes one finds $\chi_i/\chi_B \sim \rho_*$ (gyro-Bohm scaling). In linear theory, radial eigenmode structures typically scale like $\rho_*^{1/2}$, which would give a weak or null (Bohm) ρ_* dependence, whereas non-linear considerations would suggest a gyro-Bohm scaling. Hence the need for an assessment.

The finding that the actual ion conductivity indeed scales in a gyro-Bohm fashion has been obtained by a series of numerical similarity experiments. In these experiments, the input power (in the form of a given heat flux F_{in} at the inner boundary) and ρ_* were varied proportionally (keeping the ratio F_{in}/ρ_* constant), down to a value of $\rho_* = 1/200$, to test whether the profiles remain the same and the conductivity varies proportionally to ρ_* .

In order to ensure that the time averages were taken in steady state, we monitored the time

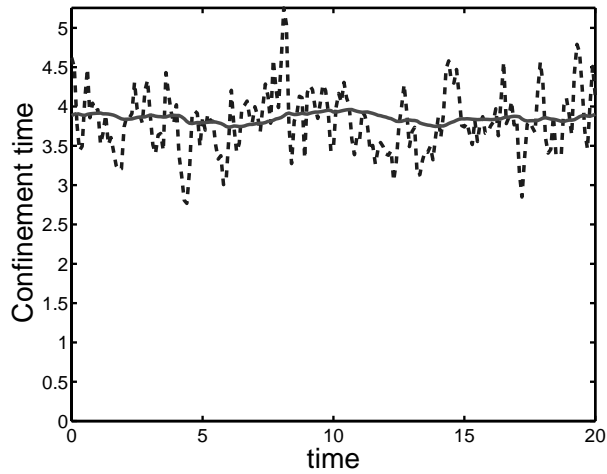


Figure 1. The two equivalent definitions of the confinement time, τ_{E1} (solid line) and τ_{E2} (dashed line), for a run at $\rho_* = 1/50$, $F_{in} = 3 \times 10^{-2}$.

evolution of two definitions of the global confinement time, $\tau_{E1} = E_{th}/F_{in}$ and $\tau_{E2} = E_{th}/F_{out}$, which are written as the ratio of the instantaneous thermal energy content E_{th} to the constant input power F_{in} and to the fluctuating instantaneous losses F_{out} , respectively. Statistical stationarity is evident from Fig. 1, where the two definitions τ_{E1} (solid line) and τ_{E2} (dashed line) are, on average, equal.

The results of the ρ_* scan experiments are summarized in Fig. 2, which shows the time averaged temperature profile, temperature gradient, local effective conductivity and temperature fluctuations, obtained at progressively smaller ρ_* (1/50, 1/100 and 1/200), and proportionally reducing the input power F_{in} from 3×10^{-2} to 7.5×10^{-3} . Figure 2 shows that by reducing ρ_* one needs proportionally less power to sustain the same gradient, and thus the conductivity is proportional to ρ_* , when expressed in Bohm units (gyro-Bohm scaling).

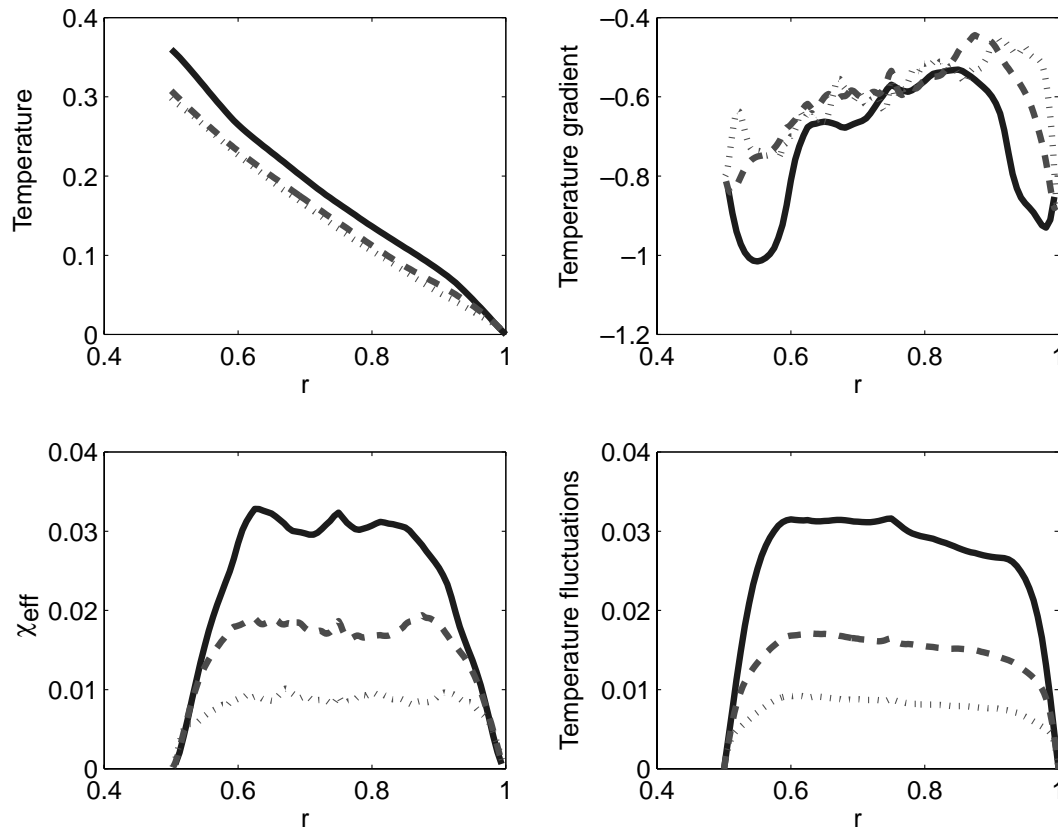


Figure 2. Similarity runs for ρ_* : solid curves, $\rho_* = 1/50$; dashed curves, $\rho_* = 1/100$; dotted curves, $\rho_* = 1/200$.

Convergence to a scaling law of the form $\chi_i/\chi_B \sim \rho_*$ as ρ_* tends to zero is especially evident when comparing the profiles obtained at $\rho_* = 1/100$ and $\rho_* = 1/200$. The $\rho_* = 1/200$ run required $\sim 10^{15}$ floating point operations and was allowed by the greater computer resources (previously [3] only $\rho_* = 1/100$ was feasible).

The gyro-Bohm nature of the observed turbulence is also apparent from direct inspection of the contour plots of the fluctuating fields [3]. More quantitative information is provided by the radial and time autocorrelation functions of the fluctuating potential, as shown in Figs 3(a) and (b). Here the abscissas are normalized to ρ_* . One can see that the halfwidths of the correlation functions, which are estimates of the radial correlation length and of the correlation time, are essentially proportional to ρ_* . As a complement, the poloidal spectra are shown in Fig. 3(c). The abscissa is $k_\theta \rho_s$. One finds that the spectra are self-similar, with a peak at $k_\theta \rho_s \approx 0.3$ for our choice of the parameters. Finally, the gyro-Bohm nature of the ITG turbulence has been found to hold over the whole range of input powers we have considered. In our studies the normalized input power F_{in}/ρ_* was varied by a factor of 100, from a minimum of $F_{in}/\rho_* = 5 \times 10^{-2}$ (which leaves the gradient very close to the ITG threshold) up to $F_{in}/\rho_* = 5$. By increasing the input power at constant ρ_* one increases the temperature gradient, and therefore the conductivity, which is also a function of the temperature gradient. This function has not yet been determined at this stage.

4. Current scaling

As a second application, the question of the plasma current scaling has been addressed. According to the empirical scaling laws, the energy confinement time is roughly proportional to the plasma current, $\tau_E \sim I_p$. This dependence can be reproduced if one assumes that the effective conductivity depends on the local safety factor to a sufficiently high power. This fact has been exploited in the phenomenological expressions of the conductivity. For example, assuming $\chi \sim q^2$ would give $\tau_E \sim I_p$ for a Bohm model [4] and $\tau_E \sim I_p^{0.8}$ for a gyro-Bohm model [5], with no dependence of τ_E on the toroidal magnetic field in the latter case. However, unlike the case of the dependence of the conductivity on ρ_* , which is a consequence of the scale separation between micro-turbulence and large scale plasma dynamics, there is no a priori reason why the q dependence should

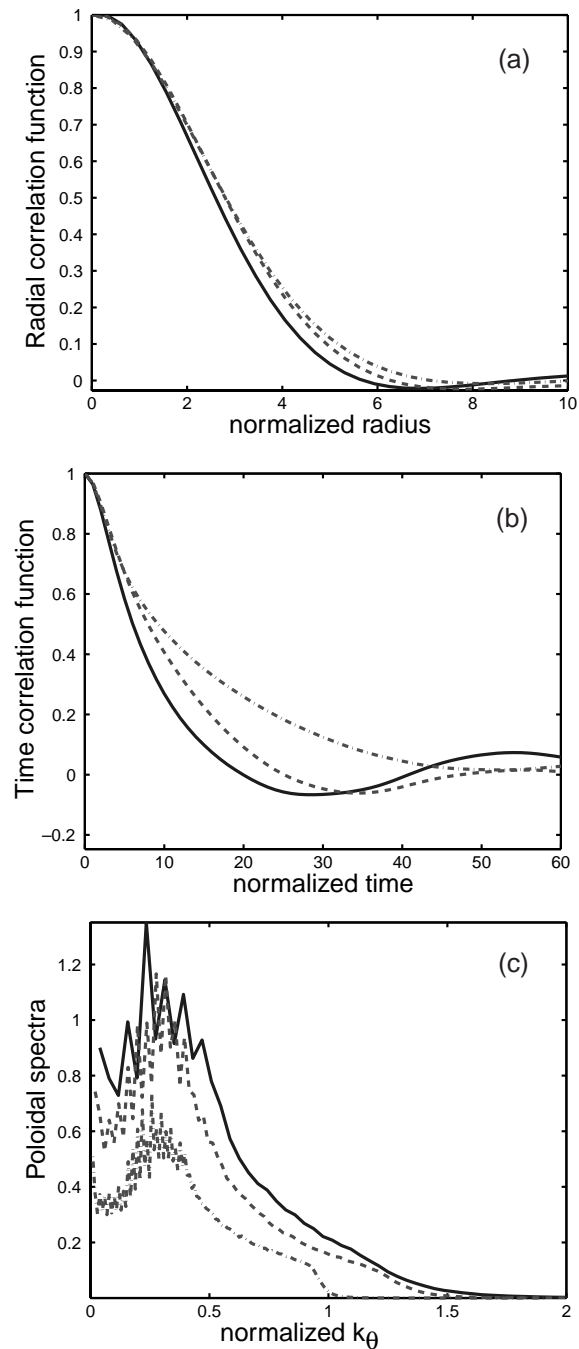


Figure 3. (a) Radial correlation functions, (b) temporal correlation functions and (c) poloidal spectra for: solid curves, $\rho_* = 1/50$; dashed curves, $\rho_* = 1/100$; chain curves, $\rho_* = 1/200$.

be monomial. Indeed, the global confinement dependence on the current can come from the co-operative effect of various parameters, such as the local q , the magnetic shear (which both change at the same time in experimental current scans) and the edge conditions.

A numerical assessment of whether the effective conductivity scales with q has been carried out for the ITG model using the similarity experiment technique, with q profiles of the form $q = q_a r^{\hat{s}}$, by changing q_a and keeping the magnetic shear \hat{s} constant and uniform in space (here $\hat{s} = 1$). The main finding is that the q dependence cannot be cast in simple monomial form, as explained below.

A first similarity test was carried out at moderate input power. It consisted in running a simulation at $q_a = 4$ and $F_{in}/\rho_* = 1.5$, which we call here the reference case (run 1), and two simulations, both at $q_a = 2$, with $F_{in}/\rho_* = 0.75$ (run 2, to test whether $\chi_i \sim q$) and $F_{in}/\rho_* = 0.375$ (run 3, to test, as an alternative, $\chi_i \sim q^2$). We recall that a dependence of at least $\chi_i \sim q^2$ is needed to reproduce the observed scaling, while the weaker $\chi_i \sim q$ dependence is essentially what results from flux tube ITG turbulence simulations [6].

The results are shown in Fig. 4, where the conductivity ratios of the reference run to both test runs are given. It is apparent that no similarity experiment gives fully satisfactory results, with $\chi_i \sim q$ being a too weak scaling and $\chi_i \sim q^2$ probably a too strong scaling. Thus, if one were to cast the q dependence as a pure monomial scaling of the form $\chi_i \sim q^\beta$, this would require $1 < \beta < 2$.

To verify this trend, a second study was performed at a higher normalized input power, with a new reference run with $q_a = 4$ and $F_{in}/\rho_* = 5$ (run 1). Now the test case $q_a = 2$, $F_{in}/\rho_* = 2.5$ (run 2) shows that $\chi_i \sim q$ is already too strong, and thus one would have to take $\beta < 1$ at higher input power (Fig. 5). The conclusion is that no simple monomial dependence of the effective conductivity on q can be used to represent all the data.

On the other hand, we note that, qualitatively, the numerical findings are consistent with the local expression

$$\chi \sim \rho_* q^\beta (R/L_T)^\gamma f_{thrs}[(R/L_T) - C_{th}/q^{\beta'}] \quad (4)$$

where $f_{thrs}[\cdot]$ is a monotonic threshold function. Note the double dependence on q characterized by two positive exponents β and β' . In general, a reduction of q (larger current) translates into a reduction of χ in two ways, via the factor q^β and through the increased threshold (factor $C_{th}/q^{\beta'}$). At smaller input power, when one works closer to threshold, the latter is more effective and gives a stronger apparent scaling than when working further from threshold.

The fact that the threshold function depends on q is confirmed by running the code in linear mode,

using a family of profiles with increasing temperature gradient and looking for the onset of the instability. The threshold was found to decrease when q is increased. Moreover, it is interesting to note that a similar behaviour is found experimentally in Tore Supra [7], where the measured electron conductivity is consistent with $\beta' = 1$, i.e. an effective threshold depending inversely on q .

Finally, as a complement to the current scaling study, we have investigated the dependence on the magnetic shear at constant current. We again chose uniform shear q profiles of the form $q = q_a r^{\hat{s}}$ with fixed $q_a = 4$. Figure 6 shows the results of three runs carried out with ‘normal’ shear values $\hat{s} = 0.25$ (dotted curve), $\hat{s} = 0.5$ (dashed curve) and $\hat{s} = 1$ (solid curve), and the same value of the normalized input power $F_{in}/\rho_* = 1.5$. Transport is only slightly reduced by varying the shear in this range. Interestingly, the fluctuation level is almost unaffected.

In experiments an increased current is usually accompanied by a broader current profile, with lower average magnetic shear. Thus the dependence on the shear and on the local q combine to determine the effective current dependence of the confinement time. A third effect, not analysed here, is the possible dependence of the edge conditions on the local q .

5. Discussion and summary

We have employed the global turbulence code ETAI3D to study the dependence of the effective conductivity on two important parameters that control ITG turbulent transport.

The ρ_* similarity studies confirm and strengthen earlier results, obtained at lower resolution, that transport has gyro-Bohm scaling in the conductivity, in the characteristic spatial and time scales and in the fluctuation level, as $\rho_* \rightarrow 0$. This behaviour is seen in all regimes of input power, which was varied by a factor of 100.

Given the importance of ITG turbulence as a transport mechanism in the ion channel and the fact that the gyro-Bohm scaling is now firmly established, we suggest that this ρ_* dependence should be explicitly incorporated in the empirical scaling laws to reduce the uncertainty in the determination of the dependence of the conductivity on the other parameters.

The dependence on plasma current was found to be more complicated. An effective scaling of the form $\chi \sim q^2$ almost works for moderate input power, while

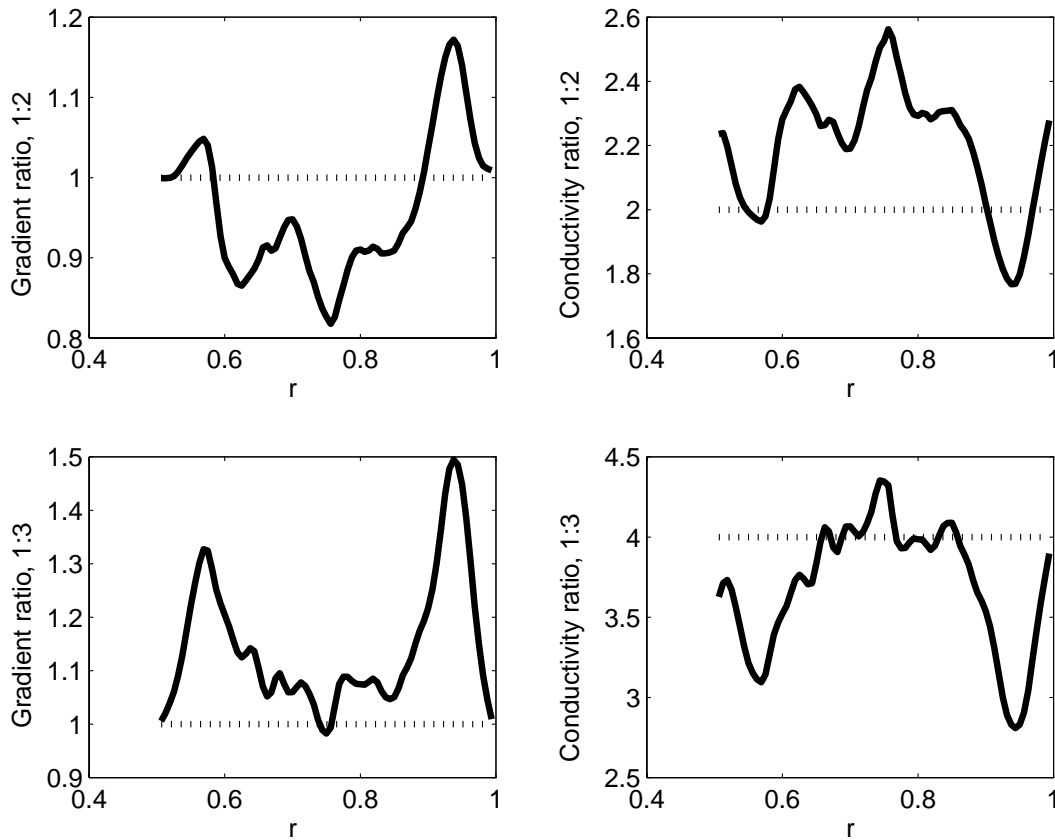


Figure 4. Temperature gradient and conductivity ratios for the q scaling study at medium forcing.

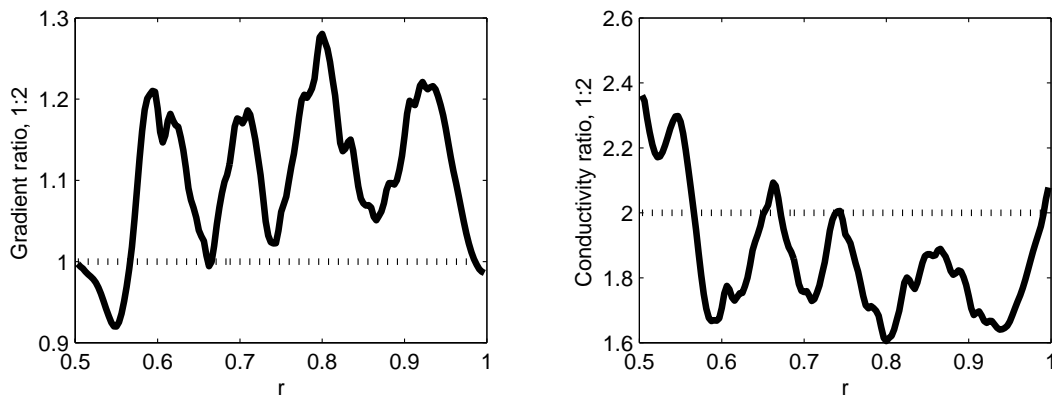


Figure 5. Temperature gradient and conductivity ratios for the q scaling study at strong forcing.

a weaker scaling holds at stronger input power. This behaviour could be traced to (at least) a double dependence of χ on the local q , one multiplicative (in the coefficient) and one indirect through the ITG threshold. At low input power, the gradient is essentially determined by the threshold and its parametric dependence.

This is valid, at least within our fluid model. One could object that, in reality, the actual threshold is determined by kinetic effects. This notion is implemented in some transport models [6], where the kinetic threshold depends weakly on q . However, one should consider the possibility that, for sufficiently high input power such that a fluid model can be

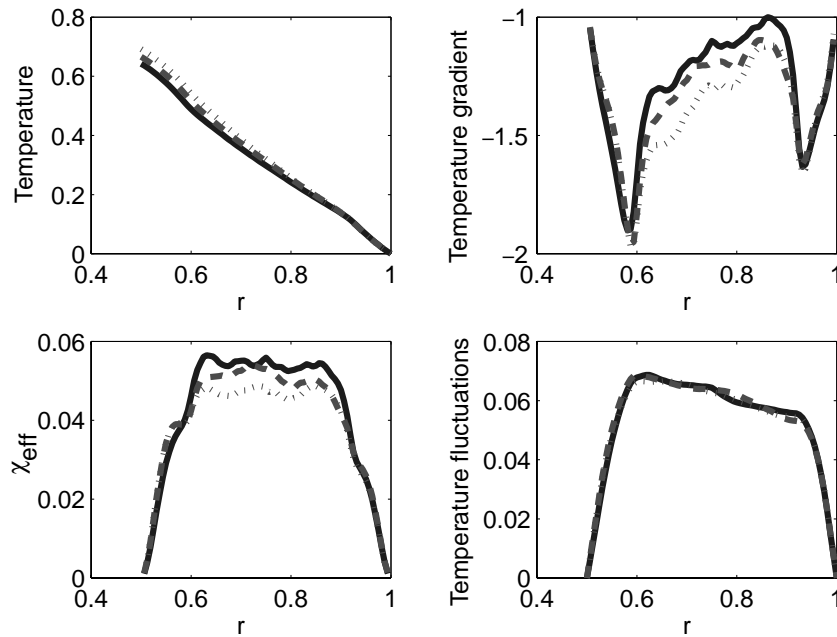


Figure 6. Shear scans at constant input power and current: solid curves, $\beta = 1$; dashed curves, $\beta = 0.5$; dotted curves, $\beta = 0.25$.

employed, the offset in the conductivity formula is determined by the fluid threshold, which is higher than the kinetic one. We also remark that a strong q dependence of the empirical threshold is observed in the electron channel.

References

- [1] ITER Physics Basis, Ch. 2: Plasma Confinement and Transport, Nucl. Fusion **39** (1999) 2175.
- [2] Jacquinot, J., et al., Nucl. Fusion **39** (1999) 235.
- [3] Ottaviani, M., Manfredi, G., Phys. Plasmas **6** (1999) 3267.
- [4] Taroni, A., Erba, M., Tibone, F., Springmann, E., Plasma Phys. Control. Fusion **36** (1994) 1629.
- [5] Ottaviani, M., Horton, W., Erba, M., Plasma Phys. Control. Fusion **39** (1997) 1461.
- [6] Kotschenreuther, M., Dorland, W., Beer, M.A., Hammett, G.W., Phys. Plasmas **2** (1995) 2381.
- [7] Hoang, G.T., et al., "Electron transport and improved confinement in Tore Supra", IAEA-CN-77/EX6/1, paper presented at 18th Conf. on Fusion Energy, Sorrento, 2000.

(Manuscript received 4 October 2000

Final manuscript accepted 19 February 2001)

E-mail address of M. Ottaviani:
mao@drfc.cad.cea.fr

Subject classification: D2, Tt; F1, Tt